PHYSICAL REVIEW B VOLUME 30, NUMBER 10 15 NOVEMBER 1984

Angle-resolved photoemission study of the electronic structure of beryllium: Bulk band dispersions and many-electron effects

E. Jensen, R. A. Bartynski, T. Gustafsson, and E. W. Plummer
Department of Physics and Laboratory for Research on the Structure of Matter, University of Pennsylvania, Philadelphia, Pennsylvania 19104

M. Y. Chou and Marvin L. Cohen
Department of Physics, University of California and Materials and Molecular Research Division, Lawrence Berkeley Laboratory, Berkeley, California 94720

Gar B. Hoflund
Department of Chemical Engineering, University of Florida, Gainesville, Florida 32611
(Received 20 July 1984)

Angle-resolved photoemission spectra from Be(0001) in the photon energy range 10—120 eV are presented and discussed. The band structure along Δ is determined and compared with our calculation using an *ab initio* self-consistent pseudopotential method in the local-density formalism. The occupied bandwidth, characterized by the Γ_1^+ symmetry point energy, is found to be 11.1 ± 0.1 eV, which is in excellent agreement with the calculated value of 11.16 eV. The most shallow occupied symmetry point on Δ, Γ_3^+, is found at 4.8 ± 0.1 eV, while the calculated value is 4.32 eV. The lowest-energy unoccupied band is in good agreement with the calculation with the exception of some extra structure near the plasmon threshold. This extra structure is associated with interaction between the excited electron and plasmons. The peak widths for photon energies below 33 eV are in reasonable agreement with widths predicted for hole lifetimes in the homogeneous electron gas.

I. INTRODUCTION

Although the electronic structure of the simple *sp*-band metals has been fairly well understood for many years, there remain some important issues to be addressed. One unresolved question is how accurately state-of-the-art band calculations can describe the ground-state properties of these metals. The answer to this question is important for defining the limitations of the widely used local-density approximation. Very recent work has shown quite good agreement.[1] Another question is how well these calculations describe excitation properties of the type observed with optical and photoemission spectroscopies. Here the agreement does not seem as good, but is still quite reasonable.[2,3] This imperfect agreement is not surprising since density functional eigenvalues do not have a formal interpretation as excitation energies.[4] This point leads to a third question: How well can these discrepancies be understood? A first step toward a full solution is provided by the calculated quasiparticle properties of the homogeneous, interacting electron gas. These properties have traditionally been considered only very near to the Fermi level, but the deeper excitations are, if anything, even more interesting. Several predictions of many-body theory for excitations of the electron gas far from the Fermi level have remained essentially untested for many years.[5,6] They include predictions of a narrowing of the occupied band, of sharp structure near the threshold for plasmon production, and of specific values for the hole and electron lifetimes which determine peak widths and sampling depths. These predictions represent a first approximation to the difference between the density functional ground-state and excitation, or quasiparticle, bands for simple metals. They are often classed together as self-energy effects. Angle-resolved photoemission allows the study of these excitations in detail.

Beryllium has many properties that make it a good choice for this kind of investigation. It is useful to study a wide-band, *sp* metal because this is the type of material for which the band calculations can be done accurately, for which the spectra are expected to be simple, and for which calculated results from the many-body theory are expected to apply. Atomic beryllium ($Z=4$) has a closed shell $(1s)^2(2s)^2$ configuration. The $2s$ and $2p$ bands hybridize in the solid state, leading to metallic behavior and a wide *sp* band. The unoccupied bands remain simple (little *d* or *f* character) for some distance above the Fermi level. The density of states at the Fermi level is very low, as explained already by Herring and Hill[7] and shown clearly, for example, in photoemission spectra from polycrystalline films.[8,9]

In this study, angle-resolved photoemission is used to determine properties of occupied and unoccupied bands of Be along Δ. These experimental results are compared with an *ab initio* pseudopotential calculation. Generally good agreement is found. The occupied band is characterized by the Γ_1^+ and Γ_3^+ symmetry point binding energies. Experimental (theoretical) values are, respectively, 11.1 ± 0.1 eV (11.16 eV) and 4.8 ± 0.1 eV (4.32 eV). The

lowest unoccupied band is also investigated in detail and found to be in good agreement with theory. A distortion in the unoccupied states near the plasmon energy, for which the shape is significantly more complex than predicted, has been reported in a previous study.[3] Finally, the measured peak widths are found to be dominated by hole lifetimes, which are close to those calculated for the electron gas. The electron lifetimes are significantly longer than predicted. These differences are attributed to the fact that electron-gas theory ignores the possibility of interband transitions, and to the fact that the electron gas is in some respects a poor approximation to Be.

The remainder of this paper is organized as follows: In Sec. II we describe the experimental and theoretical procedures, in Sec. III we present the results, in Sec. IV we discuss the main points, and in Sec. V we present the conclusions.

II. EXPERIMENTAL AND THEORETICAL METHODS

The experimental data were obtained at the Synchrotron Radiation Center at the University of Wisconsin, in Stoughton, Wisconsin. The radiation was dispersed by a toroidal grating monochromater yielding photons in the $10 < \hbar\omega < 120$-eV range.[10] The electrons were energy analyzed with a hemispherical electrostatic analyzer with an acceptance angle of $\pm 2.5°$.[11] Total-energy resolution, including electrons and photons, was typically 0.3 eV, but varied from 0.1 to 1.0 eV.

The experimental chamber is a standard μ-metal shielded stainless-steel chamber with a base pressure of 10^{-10} Torr. The chamber also includes low-energy electron diffraction (LEED) optics and a cylindrical mirror analyzer for Auger electron spectroscopy (AES) and angle-integrated photoemission measurements.

The Be(0001) sample was provided cut and mechanically polished by the Cornell Materials Science Center, Ithaca, New York. It was cleaned initially by extensive sputter-annealing cycles. Several hours of argon ion bombardment (1 keV Ar^+, 10 μA/cm^2) at room temperature were required to remove the initial oxide layer. A small remnant of oxygen, about 1% of the Be AES signal, could not be removed by this procedure. In spite of the small AES signal, prominent peaks due to oxygen were observed in the photoemission spectra at 6.5 and 8.5 eV. It was found that this remaining oxygen could be removed only by sputtering at an elevated sample temperature (between 300 and 500 °C). Final cleaning immediately prior to data acquisition consisted by sputtering for 5 min (1 keV Ar^+ and 10 μA/cm^2), maintaining the sample at 450 °C. The sample was then held at this temperature for a few minutes to anneal the damage before being allowed to cool. This procedure produced a fair quality, sixfold LEED pattern, no trace of contamination as seen by AES (less than 1% of the Be signal), and reproducible, apparently clean photoemission spectra. Only one prominent peak, near 105 eV, is then visible in AES.[12]

The crystal structure of Be is hexagonal close packed (hcp) with two atoms per unit cell. The conventional real-space unit cell is shown in Fig. 1 as is the corresponding Brillouin zone (BZ). The notation of Herring is used.[13]

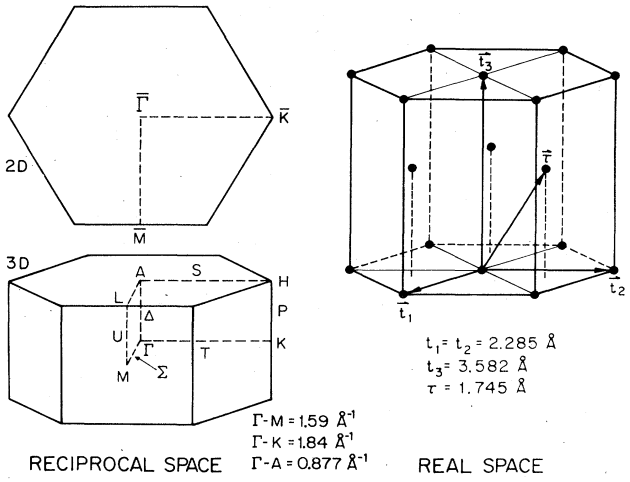

FIG. 1. Real- and reciprocal-space unit cells of hcp Be. Also shown is the surface Brillouin zone of Be(0001).

All spectra reported were taken, collecting electrons along the sample normal, using p-polarized light incident at 45° from the normal. Conservation of electronic momentum then restricts transitions to the Δ line in the Brillouin zone. Since Be has two atoms per unit cell, there are (in the absence of spin-orbit coupling) no band gaps at A (the zone boundary) in the BZ. The bands that can be observed in normal emission photoelectron spectra have Δ_1 or Δ_2 symmetry. The dipole operator does not break this symmetry and it is, therefore, convenient to unfold the bands around the A point, as is done below.

All binding energies and kinetic energies reported are referenced to $E_F = 0$. All widths reported are full widths at half maximum (FWHM).

The theoretical calculation is based on the pseudopotential approach within the local-density functional formalism.[14,15] This technique has been very successful in studying structural and dynamical properties of semiconductors and metals.[16] In the density functional theory,[4,14] the total energy of a many-electron system is considered as a functional of its density only. By using the variation principle, a one-particle Schrödinger-like equation (the Kohn-Sham equation[15]) with an effective potential is obtained. Since the exact form of the exchange-correlation functional for an inhomogeneous electron gas is still unknown, the local-density approximation (LDA) is used.[4,15] The LDA approximates locally the effective exchange-correlation energy functional with that of a uniform electron gas at the same density. The approximation is good if the density is slowly varying since the density is assumed to be uniform over the range of the exchange-correlation hole. In this calculation the functional form proposed by Hedin and Lundqvist[17] is used. Comparisons have been made using the Wigner correlation formulas[18] and only small changes in the eigenvalues were found.

The core electrons are assumed to be atomiclike, and pseudopotentials are employed to account for the interaction between the valence electrons and the ionic cores. The pseudopotentials are generated from an atomic calcu-

lation.[19] They are required to reproduce the results of the all-electron calculation, including the energy eigenvalues, eigenfunctions (outside the core region), and the excitation energies for different electronic configurations. The Kohn-Sham equation is solved self-consistently using a plane-wave basis set,[20] where plane waves with energies up to 10 Ry are included. By examining the total energy of the system, the static structural properties such as lattice constants, bulk modulus and Poisson's ratio are predicted successfully.[1] The momentum distribution (the Compton profile) is also in good agreement with experiment.[1] The eigenvalues are calculated using the self-consistent charge density at the experimental lattice constants.

III. RESULTS AND ANALYSIS

The interpretation of the experimental data is based on the independent particle approximation to the photoemission processes as described extensively elsewhere.[21,22] All many-body effects are treated within this picture as perturbations of the one-electron states.

Figure 2 shows a sequence of normal emission spectra taken at various photon energies. The stationary peak at 2.8 eV is a surface state in the Γ_3^+-Γ_4^- gap.[23] This state is discussed elsewhere.[24] The deeper, dispersive peak is the bulk transition. For $\hbar\omega < 33$ eV and $\hbar\omega > 90$ eV, a single, well-defined bulk peak is observed. However, for $33 < \hbar\omega < 90$ eV, weak, complex peaks are seen, and they are poorly approximated by a single Gaussian or Lorentzian line shape.

A. Eigenvalues and peak positions

In Figs. 3(a), 3(b), and 3(c) the results of the first step of the data analysis are summarized showing peak binding energy, peak width, and peak intensity, respectively, as a function of photon energy. In these figures the bulk peak is represented by a solid circle when a symmetric, well-defined peak is observed, or by an open circle when a weak, asymmetric peak is seen. In Fig. 3(a), the bulk peak first disperses downward, away from E_F. At $\hbar\omega = 32$ eV it reaches a maximum binding energy of 11.1 eV, which is associated with the Γ_1^+ symmetry point. It then disperses back upward, becomes broad and asymmetric, and loses intensity. The solid curve in this figure is the dispersion expected if the final-state band were a free-electron band originating 11.1 eV below E_F. Clearly, a better model is required to explain the data, but the origin of the peaks is evident even by this simple comparison.

Above 38 eV another peak starts dispersing downward,

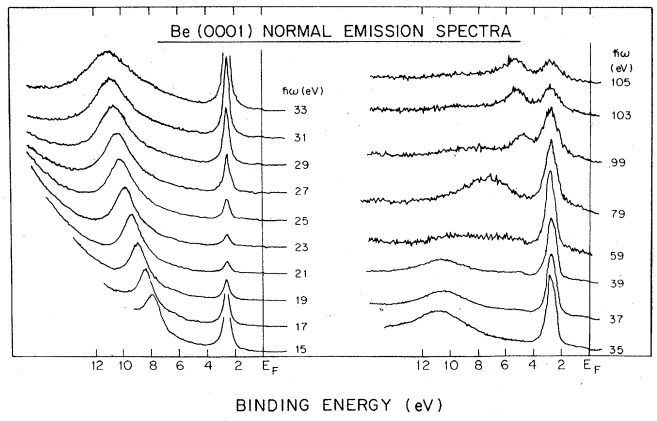

FIG. 2. Normal emission spectra of Be(0001) for different photon energies. The spectra have been rescaled vertically in an arbitrary fashion. Relative intensities may be determined from Fig. 3(b).

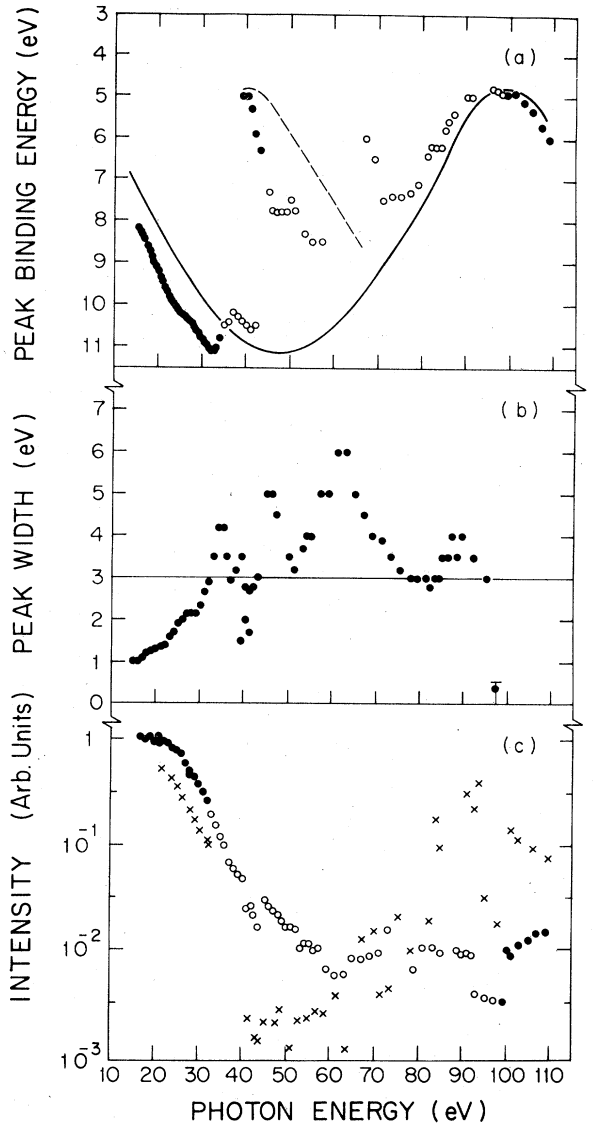

FIG. 3. (a) Peak binding energies, (b) widths, and (c) intensities as a function of photon energy. In (a) the solid line is the expected result based on direct transitions to a free-electron final state. The dashed line is obtained if the $\Delta_1 \rightarrow \Delta_1$ and $\Delta_2 \rightarrow \Delta_2$ selection rule is relaxed. In (b) the horizontal line at 3 eV differentiates somewhat arbitrarily between sharp, well-defined peaks [less than 3 eV and denoted by solid circles in (a) and (c) and Fig. 4] and broad, poorly defined peaks [open circles in (a) and (c) and Fig. 4]. The crosses in (c) are the calculated values of the direct photoexcitation transition matrix element between initial and final states (see Ref. 25). Note that the vertical scale in (c) is logarithmic.

and by 42 eV it is the dominant bulk feature. In contrast to the data below 33 eV, these data are not represented even qualitatively by a direct transition model to a free-electron final state. They lie at much smaller binding energies than such a model predicts. In Fig. 3(b) it can be seen that the emission in the range $33 < \hbar\omega < 90$ eV is dominated by broad, asymmetric peaks. Finally, above 90 eV the peak narrows and begins to track the simple free-electron final-state curve again. At $\hbar\omega = 95$ eV the peak reaches its minimum binding energy (4.8 eV), which is associated with the Γ_3^+ symmetry point on the Δ axis.

Most of the discrepancies between the data and the free-electron final-state model which occur for $\hbar\omega < 33$ eV and $\hbar\omega > 90$ eV may be removed by comparison to a more sophisticated band-structure calculation. This is done below. For $33 < \hbar\omega < 90$ eV, however, an improved single-particle calculation cannot explain the results. In order to understand these results, consider Fig. 3(c), where a plot of the peak intensity of the dominant bulk peak in the spectrum as a function of $h\nu$ is shown. The experimental points are compared to calculated values for the (square of the) direct transition matrix elements from the pseudopotential band structure. These have been multiplied by the component of the final state propagating in the direction of the surface normal and scaled to agree with the data at low photon energies.[25] This calculation indicates the strength of the transition, but it should not be compared in any detailed way with the data because only minimal consideration has been given to the transport and escape of the excited electron. Also, density-of-states effects have not been included nor have the data been corrected for a possible energy dependence of the photoelectron energy analyzer transmission. However, variations in this calculated quantity are expected to reflect the behavior of the photoelectron intensity due to direct transitions. It is clear that anomalous peaks occur only when this transition probability is very low. Other secondary effects, such as indirect transitions caused by phonons, defect or impurity scattering, and symmetry-breaking transitions due to the presence of the surface could become significant when the direct transition matrix element is small. Note that in nearly all spectra, the surface feature dominates emission from the bulk.

It is difficult to identify which of these mechanisms actually contributes to the observed emission. The high Debye temperature of Be and the relatively low photon energy at which this emission is observed indicate that the spectra should not show strong temperature dependence. It is interesting to note that some similarities with the experimental data can be observed by plotting the dispersion expected from transitions (to free-electron final states) which break the $\Delta_1 \rightarrow \Delta_1$ and $\Delta_2 \rightarrow \Delta_2$ symmetry selection rule. The results of relaxing this selection rule are shown by the dashed line in Fig. 3(a).

Having determined which peaks are associated with direct transitions and which are not, it is now possible to compare the experimentally measured band structure to the results of the pseudopotential calculation described in Sec. II. The calculated bands of Δ_1 and Δ_2 symmetry are presented in Fig. 4 as solid lines. Unoccupied bands which include a significant component of reciprocal-

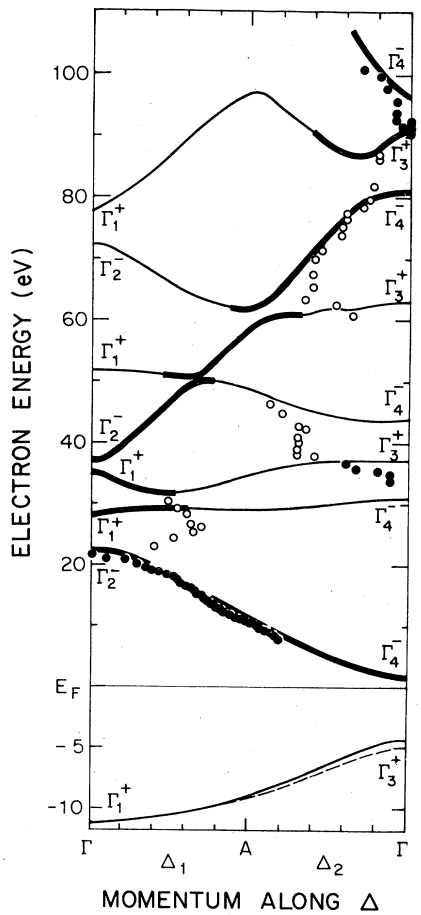

FIG. 4. Calculated and experimentally determined band structure of Be along Δ. The difference between open and solid circles is described in Fig. 3. The thicker lines denote final states, which have large plane-wave components along Δ. The dashed line is the corrected initial state (see text) used to determine the final state. Note that the vertical scale changes at E_F. A more detailed picture of the lowest unoccupied band is given in Ref. 3.

lattice vectors parallel to the sample normal (thicker lines) are expected to couple more strongly to normal photoelectron emission.

The experimentally determined occupied band is shown as a dashed line in Fig. 4. Since momentum normal to the surface is not conserved in the emission process, the method for establishing the initial bands away from the symmetry points is not unique. The following procedure is used here. The top and bottom of the band have already been determined by reading the extremal points in the plot of binding energy versus photon energy of the bulk peak from Fig. 3. This determination, which is *completely independent* of the nature of the final state, gives the bottom of the band, Γ_1^+, at 11.1 ± 0.1, eV, and the top, Γ_3^+, at 4.8 ± 0.1 eV. These values can be compared to the calculated results of 11.6 and 4.32 eV, respectively. In order to determine the final states, a representation of the initial states is needed, not just at the experimentally determined critical points, but also at arbitrary k. Therefore, the theoretical band is scaled according to the expression

$$E(k)=E_{\text{calc}}(k)-0.07[E_{\text{calc}}(k)-E_{\text{calc}}(0)]\ ,$$

so that it reproduces the experimental extrema. Here, E_{calc} is the calculated binding energy. This does not imply that the resulting empirical band is in fact the "correct" band, but only that this is the simplest way to make the small corrections to the occupied band required to determine the unoccupied bands. A value for $k_\perp$ may now be assigned to each observed transition. The unoccupied bands follow by subtracting the binding energy from the photon energy at which the transition occurs. The results of this analysis are shown in Fig. 4 with the same symbol conventions used earlier.

B. Peak widths

In Fig. 3(b) the measured peak widths are shown as a function of photon energy. For all but the very highest photon energies, the peak widths are significantly larger than the experimental resolution. The figure demonstrates, as stated several times above, that the peak behavior for $33<\hbar\omega<90$ eV is erratic, with mostly anomalously broad and asymmetric spectral features. In Sec. IV only the well-behaved peaks are discussed. For most photon energies above 95 eV, the peak widths are limited by instrument resolution. Therefore, fewer data points are given in this region in Fig. 3(b) than in Figs. 3(a) and 3(c).

IV. DISCUSSION

A. Eigenvalues and peak positions

The experimental and calculated bands can be compared in three different aspects: the Γ_1^+ symmetry point, the Γ_3^+ point, and the lowest unoccupied band. The agreement at Γ_1^+ is excellent, while the Γ_3^+ point is found about 0.5 eV deeper than predicted. Finally, the lowest unoccupied band is found to be very similar to the calculated band, except for some additional sharp structure near the plasmon energy.[3] The only other published self-consistent band calculation[26] is in excellent agreement with the present calculated eigenvalues (see Table I). The agreement with the non-self-consistent calculation by Nilsson *et al.* is only marginally worse,[27] and, also, the results by Terrell are quite reasonable.[28] Most other calculations give bandwidths of approximately 12 eV,[7,29–31] with a few yielding even higher values.[32–35] Only one falls significantly below 11 eV.[36] The Γ_3^+ point is almost always found between 4.2 and 4.4 eV.[26–31,33]

There are two possible sources of disagreement between spectroscopically derived and local-density functional bands. Firstly, the local approximation to the exchange-correlation potential could be inadequate and lead to errors. Secondly, even if nonlocal effects in the exchange-correlation potential were properly included, the resulting eigenvalues would be formally distinct from excitation energies and require correction for self-energy effects.[4] Both of these problems are quite difficult to correct for, but correction of either has given 0.5-eV improvements in the silicon band structure.[37,38] However, both effects are expected to be less important for the unoccupied bands of simple metals.

Self-energy corrections for the electron gas at the beryllium density are expected to result in a 0.3-eV shift toward lower binding energy of the Γ_1^+ point and essentially no shift into the Γ_3^+ point energy.[5] Obviously these corrections would diminish, not improve, the agreement between the data and the calculations. Attempts to include these effects properly in band calculations for Al (Ref. 39) and Ni (Ref. 40) have shown that the major effects still occur at the bottom of the band and are still small.

By definition, nonlocal effects are missing in the electron gas. We know of no quantitative estimate of the effects of this approximation on the bands of a simple metal. It can be expected that in metals these effects would be much smaller than the 0.5-eV effects seen in silicon because the spatial variation of the charge density is much less.

Overall, then, both possible causes of the observed discrepancy in the occupied band seem unlikely. Similar discrepancies have been seen for Al (Ref. 2) and Mg (Ref. 41).

The extra structure in the experimental unoccupied band visible in Fig. 4 has been attributed to a self-energy effect caused by the electron-plasmon interaction.[3] A similar distortion is predicted for the electron gas.[6] The difference between the experimental and calculated final bands is shown in Fig. 5. It is compared with the self-energy correction predicted for the electron gas (solid

TABLE I. Binding energies of occupied symmetry points.

	Symmetry point	
	Γ_1^+ (eV)	Γ_3^+ (eV)
Experiment (this work)	11.1±0.1	4.8±0.1
Theory (this work)	11.16	4.32
Theory (Wilk *et al.*, Ref. 26)	11.6	4.35
Theory (Nilsson *et al.*, Ref. 27)	11.0	4.2
Theory (Terrell, Ref. 28)	11.4	4.4

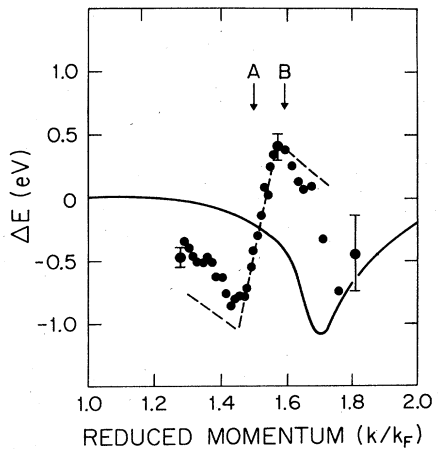

FIG. 5. Difference between calculated and experimental final-state binding energies for $\hbar\omega\lesssim 33$ eV plotted as a function of reduced momentum. The experimental points are plotted using k from Fig. 4 and then dividing by the free-electron value of k_F for Be ($=1.93$ Å^{-1}). The solid curve is the electron-gas prediction from Ref. 6. The dashed curve is the experimental results if the unscaled calculated initial states are used. See Ref. 3 for more details.

curve).[6] The predicted effect has the same magnitude, position, and width as the data but the shape of the experimental curve is significantly more complex. These differences are attributed to band-structure effects.[3] Phrased differently, the data in Fig. 5 show that the inner potential, as used, for example, in LEED structure determinations, is not a monotonic function of electron energy.

As discussed below, the location of two final-state symmetry points have also been determined. Γ_2^- is located at 21.4 ± 0.5 eV and Γ_4^- at 92 ± 1 eV above E_F. This compares to the calculated values of 21.9 and 95.4 eV, respectively. This agreement is quite satisfying.

B. Peak widths

The other interesting comparison which can be made with electron-gas results concerns the peak widths. If broadening due to defects, vibrations, etc. is neglected, the observed peak width W in an electron energy distribution can be written as[42]

$$W=[(2\Gamma_{\text{hole}})^2+(2R\Gamma_{\text{electron}})^2]^{1/2}\ . \tag{1}$$

Here, R is the ratio of the slopes $(\partial E/\partial k)$ in the initial- and final-state bands, and $\hbar/2\Gamma$ is the hole (electron) lifetime. For the transitions of interest here, $\frac{1}{10}\lesssim R\lesssim\frac{1}{3}$ (see Fig. 4) and $\Gamma_{\text{el}}\sim\Gamma_h$.[6] Therefore the peak widths are dominated by the hole contributions, at least away from the symmetry points. Any analysis is more complicated near such points. Peak widths for $\hbar\omega<33$ eV are plotted as a function of reduced momentum in Fig. 6 and compared with a calculation for hole widths in jellium.[6] The shape of the theoretical curve simply reflects the phase space available for decay. As the one-hole state moves away from E_F, more and more two-hole states become energetically accessible. The generally good agreement shows that the correct physical origin of the peak widths (i.e., the hole lifetimes) probably have been identified. The agreement is especially good for the shallow excitations, while the deeper excitations are somewhat broader than predicted. This additional width probably can be attributed to interband scattering, which is not included in the theory.

Final-state widths are more difficult to determine because the hole widths are so large. A common procedure[2] is to study the width at transitions originating from the Fermi level, where the hole contribution vanishes. Since no transitions from E_F are observed, this method is not applicable here. Instead, the photon energy dependence of transitions into final-state gaps has been investigated by plotting the height of the spectrum at a binding energy of 11.1 eV (Γ_1^+) and 4.8 eV (Γ_3^+) in Fig. 7. These transitions occur from Γ_3^+ to Γ_2^- near $\hbar\omega=32$ eV and from Γ_1^+ to Γ_4^- near $\hbar\omega=97$ eV. For infinite final-state lifetimes but finite initial-state broadening, step functions should be observed. The observed broadening is attributed to the final-state lifetime. If it is somewhat arbitrarily assumed that the broadening has a Lorentzian line shape, the symmetry points in the final state should be located at the 50% points and the separation of the 25% and 75% points in the plots in Fig. 7 should equal $2\Gamma_{\text{electron}}$. The results are surprising in that they yield $2\Gamma_{\text{electron}}\sim3$ eV at Γ_2^- and ~4 eV at Γ_4^-. This is compared to the theoretical values for the electron gas of 4—8 and 11 eV, respectively,[6] which are significantly larger than observed for Be. However, this analysis is higher simplified. It assumes that transitions to other states around the gap do not interfere, and also that the optical matrix elements are slow functions of $\hbar\omega$ or k. A proper photoemission calculation would be of obvious interest in order to test the accuracy of this procedure.

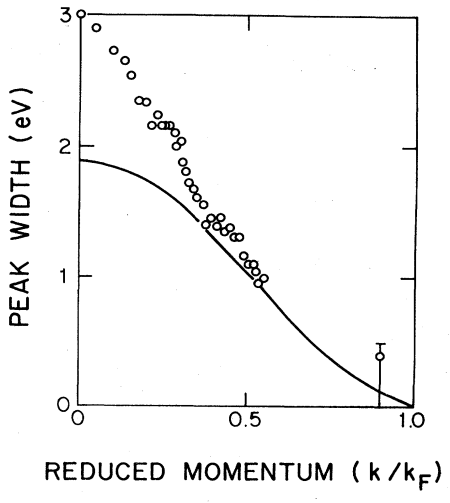

FIG. 6. Experimentally determined peak widths for $\hbar\omega\lesssim33$ eV as a function of reduced momentum. The experimental points are plotted using k from Fig. 4 and then dividing by the free-electron value of k_F for Be ($=1.93$ Å^{-1}). The solid curve is the prediction for hole-lifetime broadening in jellium from Ref. 6.

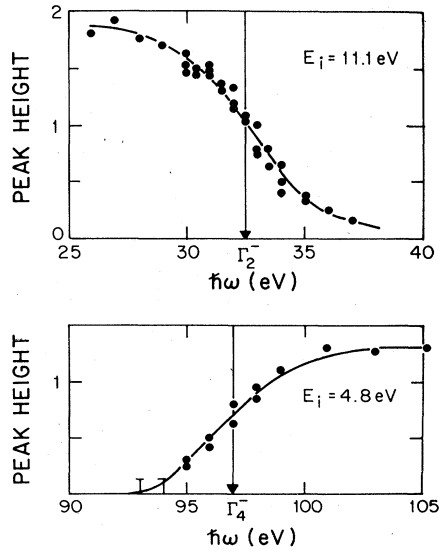

FIG. 7. Height of the peak for transitions from a binding energy of 11.1 eV as a function of photon energy in the region of transitions from Γ_1^+ to Γ_2^- (upper figure) and of transitions from a binding energy of 4.8 eV in the region of transitions from Γ_3^+ to Γ_4^- (lower figure). Final-state lifetimes are estimated from the 75—25 % width of these curves.

The narrowest peak observed in an energy distribution for transitions to Γ_4^- has a width of 0.4 eV. This value may still be resolution limited. With a knowledge of the topology of the bands around Γ_4^- and Eq. (1) it is possible to make an independent estimate of an upper limit to the electron lifetime. The result is $2\Gamma_{\text{electron}} \sim 5$ eV. Again, the analysis is complicated by the fact that both bands involved have limiting slopes of zero, but this estimate should be a better upper bound than that given in the preceding paragraph. Again, the experimental final-state lifetime is low compared to theory.

This difference is partly due to the fact that the electron-gas theory overestimates the rate of plasmon production in Be. According to electron-gas theory,[6] plasmon production accounts for more than one-half of the decay rate at the energy corresponding to Γ_4^-. This implies that the plasmon-loss satellite should be one-half as large as the primary peak.[43] In fact, in angle-integrated photoemission spectra taken near 100-eV photon energy, the plasmon-loss satellite off the valence band has only 20% of the main peak intensity. Another contributing factor to this difference is the pseudo band gap around the Fermi level in Be. This means that the rate of production of low-energy electron-hole pairs is very small, compared to a more free-electron-like metal. These data, together with the unexpectedly complex structure near the plasmon threshold,[3] show that the interaction between electrons and plasmons in Be is treated inadequately by electron-gas theory.

V. CONCLUSIONS

Angle-resolved photoemission data from Be(0001) have been presented and compared with a self-consistent pseudopotential calculation, and with the results of many-body theory for the electron gas. It is concluded that peak intensities and peak positions are well understood for those spectral features originating from direct transitions by comparison to self-consistent pseudopotential calculations. The energy of the Γ_1^+ symmetry point is predicted correctly but there is a 0.5-eV discrepancy at the Γ_3^+ symmetry point. The nature of this discrepancy is not consistent with those expected from self-energy or nonlocal exchange-correlation corrections. The lowest unoccupied band is found experimentally to be in good agreement with single-particle theory, except for some extra structure near the onset of plasmon creation.[3] When dipole cross sections are low, effects other than direct transitions become important and can actually dominate bulk emission for a large range of photon energies. The photoemission peak widths are dominated by hole lifetimes, which are fairly well predicted by electron-gas theory. Electron lifetimes in Be appear to be significantly underestimated by this theory which is partly attributed to an overestimate of the rate of plasmon production.

ACKNOWLEDGMENTS

We would like to thank D. Fowler, J. Blakely, and B. Addis of the Cornell Materials Science Center for preparing and providing the sample. We thank D. Cox and A. Baddorf as well as the staff at the Synchrotron Radiation Center for experimental assistance. This work was supported by the National Science Foundation Materials Research Laboratory program under Grant No. DMR 82-16718. The storage ring is supported by the National Science Foundation under Grant No. DMR 80-20164. This work was also supported by the National Science Foundation Grant No. DMR 83-19024 and by the Director, Office of Energy Research, Office of Basic Energy Sciences, Materials Sciences Division of the U. S. Department of Energy under Contract No. DE-AC03-76SF00098.

[1]P. K. Lam and M. L. Cohen, Phys. Rev. B **24**, 4224 (1981); M. Y. Chou, P. K. Lam, and M. L. Cohen, *ibid.* **28**, 4179 (1983); **28**, 1696 (1983).

[2]H. J. Levinson, F. Greuter, and E. W. Plummer, Phys. Rev. B **27**, 727 (1983).

[3]E. Jensen, R. A. Bartynski, T. Gustafsson, and E. W. Plummer, Phys. Rev. Lett. **52**, 2172 (1984).

[4]L. Hedin and S. Lundqvist, in *Solid State Physics,* edited by F. Seitz, D. Turnbull, and H. Ehrenreich (Holt, Reinhardt and Winston, New York, 1969), Vol. 23, p. 1.

[5]L. Hedin, Phys. Rev. **139A**, 796 (1965).

[6]B. I. Lundqvist, Phys. Status Solidi **32**, 273 (1969).

[7]C. Herring and A. G. Hill, Phys. Rev. **58**, 132 (1940).

[8]T. Gustafsson, G. Brodén, and P. O. Nilsson, J. Phys. F **4**, 2351 (1974).

[9]H. Höchst, P. Steiner, and S. Hüfner, Phys. Lett. **60A**, 69 (1977).

[10]B. P. Tonner, Nucl. Instrum. Methods **172**, 133 (1980).

[11]C. L. Allyn, T. Gustafsson, and E. W. Plummer, Rev. Sci. Instrum. **49**, 1197 (1978).

[12]Recently, H. Maguire [Solid State Commun. **45**, 71 (1983)] has claimed that an annealed Be surface has two prominent Auger peaks. Our data, as well as those of L. H. Jenkins and D. M. Zehner [Solid State Commun. **12**, 1149 (1973)], disagree with this observation.

[13]C. Herring, J. Franklin Inst. **233**, 525 (1942).

[14]P. Hohenberg and W. Kohn, Phys. Rev. **136B**, 864 (1964).

[15]W. Kohn and L. J. Sham, Phys. Rev. **140A**, 1133 (1965).

[16]M. L. Cohen, Phys. Scr. **T1**, 5 (1982); M. T. Yin and M. L. Cohen, Phys. Rev. B **26**, 3259 (1982); **26**, 5668 (1982).

[17]L. Hedin and B. I. Lundqvist, J. Phys. C **4**, 2064 (1971).

[18]E. Wigner, Phys. Rev. **46**, 1002 (1934).

[19]D. R. Hamann, M. Schlüter, and C. Chiang, Phys. Rev. Lett. **43**, 1494 (1979).

[20]J. Ihm, A. Zunger, and M. L. Cohen, J. Phys. C **12**, 4409 (1979); **13**, 3095(E) (1980).

[21]E. W. Plummer and W. Eberhardt, Adv. Chem. Phys. **49**, 533 (1982).

[22]F. J. Himpsel, Adv. Phys. **32**, 1 (1983).

[23]U. O. Karlsson, S. A. Flodström, R. Engelhardt, W. Gadeke, and E. E. Koch, Solid State Commum. **49**, 711 (1984).

[24]R. A. Bartynski, E. Jensen, T. Gustafsson, and E. W. Plummer (unpublished).

[25]The calculated intensity denoted by $\times$ in Fig. 3(c) is given by

$$I_{\text{calc}} \propto \sum_{\vec{G}_\perp} |A(\vec{G}_\perp)|^2 |M_{fi}|^2 ,$$

where M_{fi} is the dipole matrix element for the transition between initial and final Bloch states ψ_i and ψ_f. ψ_f may be decomposed as

$$\psi_f = e^{i\vec{k}\cdot\vec{r}} \sum_{\vec{G}} A(\vec{G}) e^{i\vec{G}\cdot\vec{r}} ,$$

thus defining $A(\vec{G})$. The summation over $\vec{G}$ is to be carried out only over those reciprocal-lattice vectors that fall along the sample normal.

[26]L. Wilk, W. R. Fehlner, and S. H. Vosko, Can. J. Phys. **58**, 266 (1978).
[27]P. O. Nilsson, G. Arbman, and T. Gustafsson, J. Phys. F **4**, 1937 (1974).
[28]J. H. Terrel, Phys. Rev. **149**, 526 (1966).
[29]J. H. Tripp, P. M. Everett, W. L. Gordon, and R. W. Stark, Phys. Rev. **180**, 669 (1969).
[30]S. T. Inou and J. Yamashita, J. Phys. Soc. Jpn. **35**, 677 (1973).
[31]T. L. Loucks and P. H. Cutler, Phys. Rev. **133A**, 819 (1963).
[32]R. Jaques, Cah. Phys. **70**, 1 (1956); **71—72**, 31 (1956).
[33]M. Taut, Phys. Status Solidi B **54**, 149 (1972).
[34]S. Chatterjee and P. Sinha, J. Phys. F **5**, 2089 (1975).
[35]R. Dovesi, C. Pisani, F. Ricca, and C. Roetti, Phys. Rev. B **25**, 3731 (1982).
[36]J. F. Cornwell, Proc. R. Soc. London, Ser. A **261**, 551 (1961).
[37]G. P. Kerker, Phys. Rev. B **24**, 3468 (1981).
[38]C. S. Wang and W. E. Pickett, Phys. Rev. Lett. **51**, 597 (1983).
[39]G. Arbman and U. von Barth, J. Phys. F **5**, 1155 (1975).
[40]R. E. Watson, J. F. Herbst, L. Hodges, B. I. Lundqvist, and J. W. Wilkins, Phys. Rev. B **13**, 1463 (1976).
[41]R. A. Bartynski, R. H. Gaylord, T. Gustafsson, and E. W. Plummer (unpublished).
[42]J. B. Pendry, in *Photoemission and the Electronic Structure of Surfaces,* edited by B. Feuerbacher, B. Fitton, and R. F. Willis (Wiley, New York, 1978), p. 64. A similar, but not identical, expression has been derived by J. A. Knapp, F. J. Himpsel, and D. E. Eastman, Phys. Rev. B **19**, 4952 (1979). The differences are unimportant here.
[43]W. J. Pardee, G. D. Mahan, D. E. Eastman, R. A. Pollak, L. Ley, F. R. McFeely, S. P. Kowalczyk, and D. A. Shirley, Phys. Rev. B **11**, 3614 (1975).